Title

Metabolomic Profiles of Human Glioma Inform Patient Survival.

Journal

Antioxidants & Redox Signaling, 39(13-15)

Authors

Scott, Andrew
Correa, Luis
Edwards, Donna
et al.

Publication Date

2023-11-01

DOI

10.1089/ars.2022.0085

Peer reviewed

ANTIOXIDANTS & REDOX SIGNALING
Volume 39, Numbers 13–15, 2023

DOI: 10.1089/ars.2022.0085

FORUM REVIEW ARTICLE

Metabolomic Profiles of Human Glioma Inform Patient Survival

Andrew J. Scott,[1,2] Luis O. Correa,[3] Donna M. Edwards,[1] Yilun Sun,[4] Visweswaran Ravikumar,[5] Anthony C. Andren,[6] Li Zhang,[6] Sudharsan Srinivasan,[7] Neil Jairath,[1] Kait Verbal,[7] Karin Muraszko,[7] Oren Sagher,[7] Shannon A. Carty,[2,8] Shawn Hervey-Jumper,[9] Daniel Orringer,[10] Michelle M. Kim,[1] Larry Junck,[11] Yoshie Umemura,[11] Denise Leung,[11] Sriram Venneti,[12] Sandra Camelo-Piragua,[12] Theodore S. Lawrence,[1,2] Joseph E. Ippolito,[13,14] Wajd N. Al-Holou,[7] Prakash Chinnaiyan,[15,16] Jason Heth,[7] Arvind Rao,[1,2,5,17] Costas A. Lyssiotis,[2,6,18] and Daniel R. Wahl[1,2]

Abstract

Aims: Targeting tumor metabolism may improve the outcomes for patients with glioblastoma (GBM). To further preclinical efforts targeting metabolism in GBM, we tested the hypothesis that brain tumors can be stratified into distinct metabolic groups with different patient outcomes. Therefore, to determine if tumor metabolites relate to patient survival, we profiled the metabolomes of human gliomas and correlated metabolic information with clinical data.

Results: We found that isocitrate dehydrogenase-wildtype (IDHwt) GBMs are metabolically distinguishable from IDH mutated (IDHmut) astrocytomas and oligodendrogliomas. Survival of patients with IDHmut gliomas was expectedly more favorable than those with IDHwt GBM, and metabolic signatures can stratify IDHwt GBMs subtypes with varying prognoses. Patients whose GBMs were enriched in amino acids had improved survival, while those whose tumors were enriched for nucleotides, redox molecules, and lipid metabolites fared more poorly. These findings were recapitulated in validation cohorts using both metabolomic and transcriptomic data.

Innovation: Our results suggest the existence of metabolic subtypes of GBM with differing prognoses, and further support the concept that metabolism may drive the aggressiveness of human gliomas.

Conclusions: Our data show that metabolic signatures of human gliomas can inform patient survival. These findings may be used clinically to tailor novel metabolically targeted agents for GBM patients with different metabolic phenotypes. *Antioxid. Redox Signal.* 39, 942–956.

Keywords: glioma, glioblastoma, metabolomics, IDH, astrocytoma, oligodendroglioma, oxidative stress, 2-hydroxyglutarate, recurrence

Departments of [1]Radiation Oncology, [2]Rogel Cancer Center, and [3]Immunology Graduate Program, University of Michigan, Ann Arbor, Michigan, USA.
[4]Department of Population and Quantitative Health Sciences, Case Western Reserve University, Cleveland, Ohio, USA.
Departments of [5]Computational Medicine and Bioinformatics, [6]Molecular & Integrative Physiology, [7]Neurosurgery, and [8]Internal Medicine, University of Michigan, Ann Arbor, Michigan, USA.
[9]Department of Neurological Surgery, University of California, San Francisco, San Francisco, California, USA.
[10]Department of Neurosurgery, New York University Langone Health, New York, New York, USA.
Departments of [11]Neurology and [12]Pathology, University of Michigan, Ann Arbor, Michigan, USA.
Departments of [13]Biochemistry and Molecular Biophysics and [14]Radiology, Washington University School of Medicine, St. Louis, Missouri, USA.
[15]Department of Radiation Oncology, Beaumont Health, Royal Oak, Michigan, USA.
[16]Oakland University William Beaumont School of Medicine, Rochester, Michigan, USA.
[17]Department of Biostatistics, University of Michigan, Ann Arbor, Michigan, USA.
[18]Division of Gastroenterology and Hepatology, Department of Internal Medicine, University of Michigan, Ann Arbor, Michigan, USA.

An earlier draft of this article was posted as a preprint at medRxiv: www.medrxiv.org/content/10.1101/2022.06.04.22275972v1.full.

Innovation

We do not understand how metabolites mediate cancer prognosis and treatment responses. In this article, we measure tumor metabolite levels in dozens of gliomas to create one of the largest datasets linking human glioma metabolite levels to individual patient outcome data. We find numerous metabolites and metabolic pathways that correlate with aggressive clinical behavior and confirm our findings in external datasets. This work suggests the existence of numerous glioblastoma metabolic subtypes with different prognoses that could benefit from individualized treatment strategies.

Introduction

Glioblastoma (GBM) is the most common invasive primary brain tumor and nearly uniformly fatal, despite surgical resection and subsequent standard-of-care chemoradiation. While therapeutic intervention has initial efficacy, tumors invariably recur and become resistant to treatment. Thus, there is an urgent need to identify and target molecular mediators of this resistance. While the therapy resistance and aggressiveness of GBM have been explored at genomic and transcriptomic levels, less is known about the metabolic mediators of therapy-resistant phenotypes.

Altered metabolism is a hallmark of cancers including GBM (Hanahan, 2022), and metabolic rewiring is critical for tumor cells to undergo conversion to aggressive and treatment-resistant phenotypes. Tumor metabolism is influenced by both cancer cell-intrinsic information (genome, epigenome, proteome, post-translational modifications) and cell-extrinsic cues from the tumor microenvironment.

Given that targeting metabolism has a history of success in a variety of cancers, targeting the metabolic phenotypes of GBM cells may represent an effective treatment strategy (Scott et al., 2021). Indeed, early data from several metabolically targeted therapies for GBM patients have yielded promising outcomes (Allen et al., 2019; Shenouda et al., 2020).

Understanding the metabolic phenotypes of gliomas could also provide information about tumor aggressiveness and patient prognosis. Altered expression of metabolic enzymes or imaging-defined glucose uptake can inform prognosis in a variety of cancers, including glioma (Schwarz et al., 2007; Suchorska et al., 2015; Wang et al., 2017, 2019). Metabolite levels themselves can distinguish low-grade and high-grade gliomas, and suggest that GBMs favor anabolic metabolism and heterotrophy (Chinnaiyan et al., 2012; Prabhu et al., 2019). This biology was codified in the 2016 WHO classification of gliomas, which defined three primary types of adult infiltrating gliomas (Louis et al., 2016; Tesileanu et al., 2022).

Gliomas with a mutation in isocitrate dehydrogenase (IDH) are classified as either IDH mutant astrocytomas (IDHmut astro) or IDH mutant oligodendrogliomas (IDHmut oligo). Patients with IDHmut gliomas typically live longer and respond better to treatment than patients with IDH wildtype diffuse infiltrating gliomas, which are primarily glioblastomas (IDHwt GBM). Whether metabolomic profiles can provide information regarding GBM patient outcome remains uncertain.

To address this question, we measured the metabolomes of 69 patient gliomas (Fig. 1), and found that tumors robustly cluster into IDHmut and IDHwt status based on metabolic profiles. IDHmut gliomas further separate high-grade (grade 4 astrocytoma) from lower grade tumors (grades 2 and 3 astrocytomas and oligodendrogliomas).

Further analyses of IDHwt GBM tumors reveal distinct metabolic subtypes with different patient survival times. We found no relation of these subtypes to known survival predictors, suggesting that metabolism can influence GBM progression independently of these factors. Taken together, these findings suggest the existence of discrete metabolic GBM subtypes and may pave the way for therapies targeting metabolic pathway activity to improve patient outcomes.

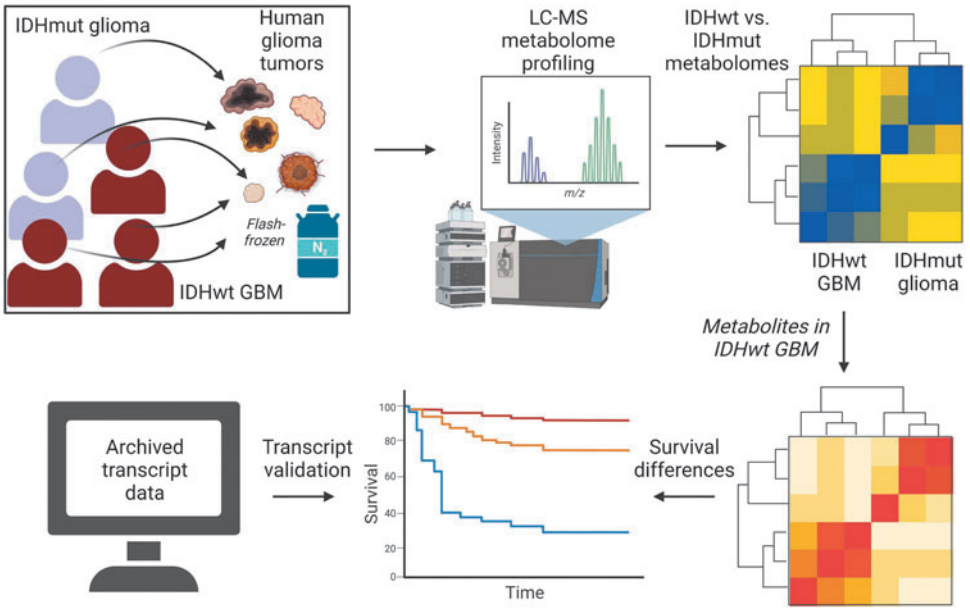

FIG. 1. Summary of study. Flash-frozen glioma samples were assessed for metabolite levels by LC-MS and grouped based on metabolomic profiles. Matching metabolomic datasets with patient information revealed survival differences among these groups. Analyses of archived gene expression data for related metabolic genes were then used to validate these findings. LC-MS, liquid chromatography-mass spectrometry.

Table 1. Patient Characteristics

Total cohort $n=69$	
IDH mutant oligodendroglioma, $n=20$	
Age	38.6 ± 17.5
Sex	Male 55%, female 45%
Extent of resection	GTR 50%, NTR 50%
Performance status	1.0 ± 0.75
Receipt of radiation	75.0%
Receipt of alkylating chemotherapy	77.8%
IDH mutant astrocytoma, $n=9$	
Age	34.0 ± 11.8
Sex	Male 44%, female 56%
Extent of resection	GTR 33.3%, NTR 67.7%
Performance status	1.0 ± 1.0
MGMT methylation status	Methylated 50.0%
Receipt of radiation	85.7%
Receipt of alkylating chemotherapy	67.7%
IDHwt GBM, $n=40$	
Age	59.8 ± 12.6
Sex	Male 64.1%, female 36.9%
Extent of resection	GTR or NTR 72.5%, STR 27.5%
Performance status	1.0 ± 1.0
MGMT methylation status	Methylated 37.5%
Receipt of radiation	96.3%
Receipt of alkylating chemotherapy	97.4%

Resected tumor samples stored in the University of Michigan Brain Tumor Bank were matched with patient medical records to determine the indicated information. Age and performance status are shown as median ± interquartile range.

GBM, glioblastoma; IDH, isocitrate dehydrogenase; MGMT, O^6-methylguanine-DNA methyltransferase.

Results

Metabolomic profiling distinguishes IDHmut from IDHwt gliomas

Using the University of Michigan Brain Tumor Bank, we identified 69 flash-frozen glioma samples with sufficient tissue for metabolomic analysis. All samples were deemed to contain ≥70% viable tumor content at time of resection after quality assurance by a clinical neuropathologist (S.V. and S.C.-P.). Clinical data associated with these tumor samples were then obtained from the medical record. This cohort (Table 1, Fig. 2 and Supplementary Data S1–S2) contained IDHmut oligo (29%), IDHmut astro (13%), and IDHwt GBMs (58%), all of which were molecularly defined (Louis et al., 2021).

Overall median survival, sex ratios, and O^6-methylguanine-DNA methyltransferase (MGMT) promoter methylation status of all three groups were as expected with median survival times of ∼11 years for IDHmut oligo, 7 years for IDHmut astro, and 1.6 years for IDHwt GBMs (Eckel-Passow et al., 2015). This longer survival time for patients with IDHmut tumors reflects the known slower growth, and improved treatment responses of IDHmut astro and IDHmut oligo compared with IDHwt GBMs (Tesileanu et al., 2022).

All patients were treated with some extent of resection (as opposed to biopsy alone) due to the requirement of sufficient tissue for banking. Within this cohort, 63% of patients with IDHmut astro, 67% of patients with IDHmut oligo, and 95% of those with IDHwt GBMs received both radiation therapy (RT) and chemotherapy, typically temozolomide (TMZ), at some point after resection.

We first asked whether metabolomic information from our tumor samples would be of sufficient quality to discriminate between known tumor subtypes (*i.e.,* IDHmut astro and IDHmut oligo *vs.* IDHwt GBMs). We extracted polar metabolites from each tumor sample and performed quantification by liquid chromatography-mass spectrometry (LC-MS) as described previously (Lee et al., 2019). With this method, we determined relative abundances of >200 compounds comprising central carbon, nucleotide, and amino acid (AA) metabolism.

To visualize whether our high-dimensional metabolite information was sufficient to group tumor samples based on their molecular subtype, we performed uniform manifold approximation and projection (UMAP) analysis. UMAP analysis revealed that IDHwt GBMs tend to separate from IDHmut gliomas, while IDHmut subsets (astrocytoma and oligodendroglioma) are more metabolically similar (Fig. 3A).

When levels of tumor metabolites across all glioma patients were analyzed by unsupervised hierarchical clustering, two distinct metabolomic groups were immediately apparent, with one cluster representing IDHwt GBM, and the other representing IDHmut astrocytoma and oligodendroglioma (Fig. 3B and Supplementary Fig. S1). This is consistent with our UMAP analysis (Fig. 3A). Mutations of IDH, typically at an arginine residue required for substrate recognition, cause an accumulation of 2-hydroxyglutarate [2HG (Dang et al., 2009; Hartmann et al., 2009; Lai et al., 2011; Parsons et al., 2008)].

As expected, the levels of 2HG were 10- to 50-fold higher in IDHmut tumors than in IDHwt GBMs (Fig. 3C). The role of 2HG in IDHmut gliomas is well established and supports our observations of increased 2HG in tumors from IDHmut

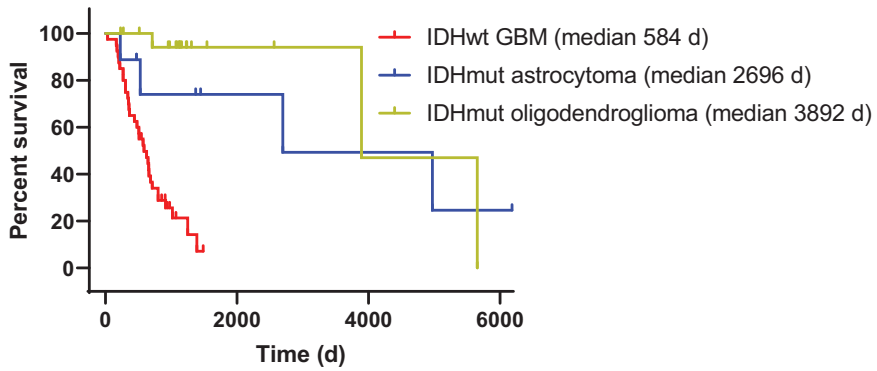

FIG. 2. Overall survival times for glioma patients. The Kaplan–Meier curves of overall survival times for glioma patients corresponding to tissue samples acquired from the University of Michigan Brain Tumor Bank with the indicated tumor types are shown. Patients with unknown survival times were censored at time of last follow-up.

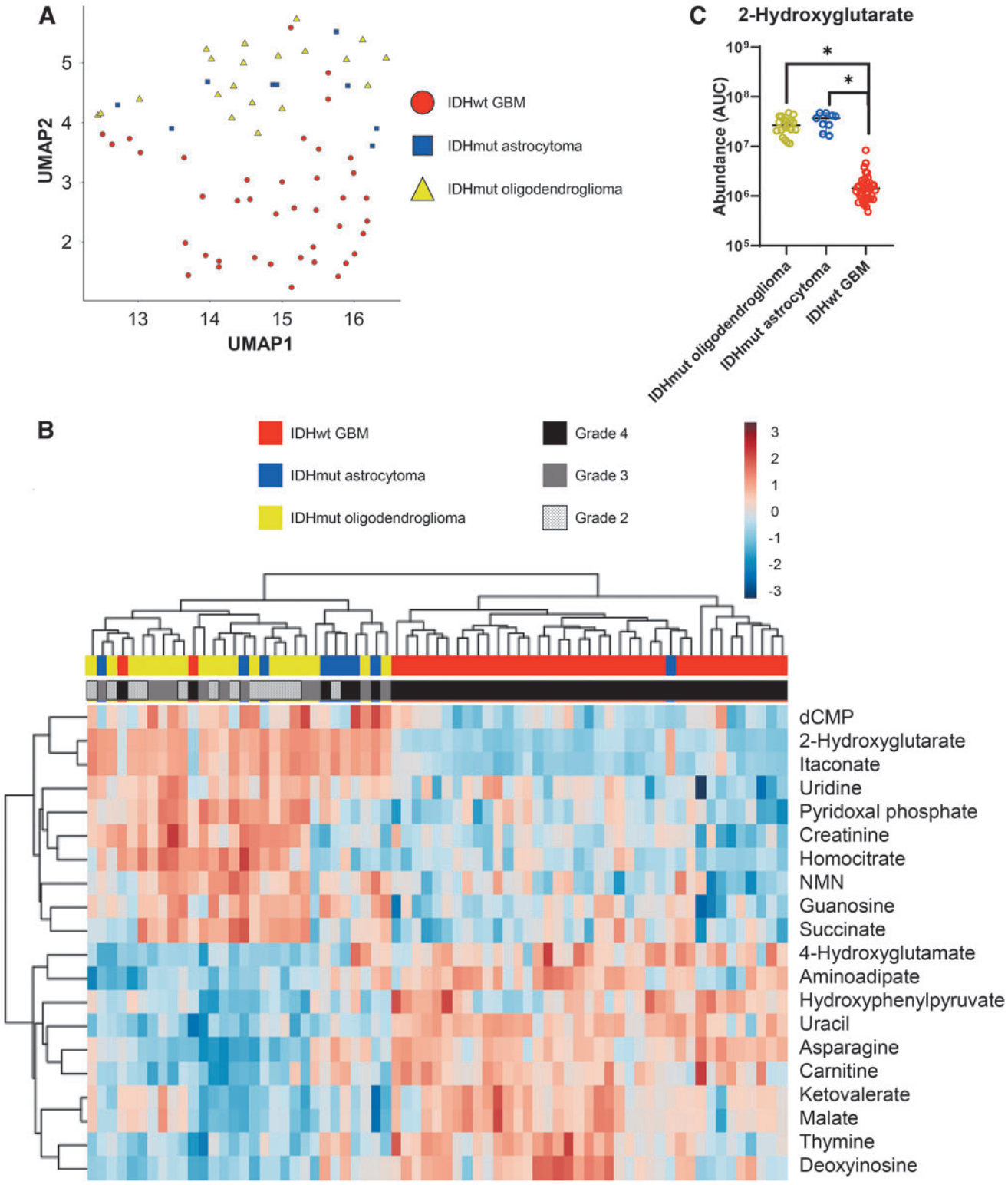

FIG. 3. Metabolomics distinguishes IDHmut from IDHwt gliomas. (A) Metabolite levels of tumors from glioma patients were measured by LC-MS, and then assessed by UMAP. **(B)** Metabolite levels were assessed by data reduction with Binner followed by unsupervised hierarchical clustering. Color scale indicates log-transformed values of data points after normalization to the median AUC of each compound. **(C)** Levels of 2HG were determined by measuring LC-MS AUCs matched to ion fragmentation data. $*p < 0.0001$, unpaired t test. AUC, area under the curve; UMAP, uniform manifold approximation and projection.

glioma patients. Surprisingly, our method identified several other metabolites, including itaconate, citramalate, and ketoleucine, which were elevated to a similar magnitude to 2HG in IDHmut tumors (Supplementary Fig. S1). These findings could hint at interesting new biology in IDHmut gliomas, or they could be mis-called metabolites due to their chemical similarity to 2HG (*e.g.,* similar fragmentation patterns and retention times on chromatography).

To discriminate between these possibilities, we processed our data using Binner (Kachman et al., 2019), which identified isobaric overlaps of 2HG with citramalate; and itaconate with ketoleucine. We confirmed similar retention times, and identical ion transitions for itaconate and ketoleucine (Supplementary Data S3). Citramalate and 2HG had similar retention times and parent ions but different ion transitions (Supplementary Data S3).

Normalized ion counts are found in Supplementary Data S1. After this additional processing of LC-MS data, IDHwt GBMs remained distinct from IDHmut gliomas (Fig. 3B). Together, these data show that our tumor metabolomic data are of sufficient quality to discriminate known molecular subtypes of glioma. With this quality assurance step in hand, we then used these data to explore novel biology within IDHmut gliomas and IDHwt GBMs.

To further explore metabolic differences between tumor types, we found that $\sim 50\%$ of detected metabolites differed in IDHwt GBM compared with IDHmut gliomas (combined astrocytoma and oligodendroglioma; Supplementary Fig. S2A). Of note, the pyrimidine breakdown products uracil and thymine are markedly elevated in IDHwt GBM compared with IDHmut gliomas, perhaps reflective of the increased demand for pyrimidines in IDHmut tumors (Shi et al., 2022). We also identified a variety of metabolites with abundance differences with $p < 0.05$ between IDHmut astro and IDHmut oligo (Supplementary Fig. S2B).

After surgical resection, gliomas are typically treated with RT and chemotherapy, which suppress tumor growth by inducing reactive oxygen species and DNA damage. Having observed different metabolite levels across different types of gliomas, we asked if metabolites related to the regulation of oxidative stress could serve as potential biomarkers and/or therapeutic targets. Therefore, we examined ratios of oxidized and reduced nicotinamide adenine dinucleotide (NAD/NADH) and glutathione (GSH/GSSG).

Notably, neither NAD/NADH ratios nor GSH/GSSG ratios differed significantly across tumor types, nor correlated with patient survival time (Supplementary Fig. S3A–F). We did observe that cystathionine, an intermediate in the transsulfuration pathway used to generate antioxidants from one-carbon metabolism, is elevated in IDHmut astro compared with IDHmut oligo (Supplementary Fig. S2B). It is possible that the labile nature of these metabolites caused degradation or oxidation during tissue storage, which obscured some correlations with patient survival and/or tumor type.

Grade 4 IDHmut astro have a worse prognosis than grade 2 or 3 IDHmut astro, but the prognostic difference between grade 2 and 3 IDHmut gliomas is uncertain in the era of molecularly defined tumors (Brat et al., 2020). Notably, grade 4 IDHmut astro clustered together based on their metabolomic profile and were separate from lower grade 2 and 3 tumors, which remained intermixed (Fig. 3B). While IDHmut grade 4 astrocytomas had similar levels of 2HG to lower grade IDH mutant tumors, their levels of asparagine and several other metabolites were more similar to IDHwt GBMs than to lower grade IDHmut tumors.

Notably, hierarchical clustering could not discriminate between grade 2 or grade 3 IDHmut tumors (Fig. 3B) with any of the 12 different linkage/distance algorithm combinations available in MetaboAnalyst (Euclidian, Pearson, Minkowski distance measurements; complete, average, single, Ward linkage methods). All 12 distance-linkage method combinations available (not shown) robustly separated grade 4 gliomas from lower grade (2/3) tumors while failing to separate grade 2 from grade 3. This suggests that either grade 2 and 3 gliomas cannot be metabolically distinguished with our LC-MS methods, or there is a need for a more robust method to categorize gliomas into grades 2 and 3 than the histological examinations used at present.

We also noted that two IDHwt GBMs clustered with low-grade IDHmut tumors (Fig. 3B). This clustering was not due to alternative IDH mutations missed by immunohistochemistry, as 2HG levels were similar to other IDHwt GBMs. Rather, these two tumors had similar levels of succinate, creatinine, and other metabolites to the IDHmut tumors.

Additional investigation of these two unusual GBM cases found survival times substantially longer than the 1.5-year median for GBM, similar to IDHmut gliomas. One patient in their early fifties survived 4 years beyond diagnosis, and the other (early twenties, far below median age of 65 years) is still alive 5.5 years after diagnosis at the time of writing. A single IDHmut grade 4 astrocytoma metabolically clustered with IDHwt GBMs.

Metabolomics-based clustering bins GBM patients into groups with different prognoses

The data above confirmed that IDHwt GBMs have a metabolic phenotype distinct from IDHmut gliomas, and suggested that our data were of sufficient quality to investigate less understood metabolic pathways in glioma. Outcome for GBM is dramatically worse than that for IDH mutant tumors. This poor survival rate may be at least partially due to metabolic phenotype (Chinnaiyan et al., 2012; Kesarwani et al., 2019; Scott et al., 2021), and we and others have demonstrated that targeting metabolism in GBM can improve survival in animal models and is under investigation in patients (Schoenfeld et al., 2017; Shenouda et al., 2020; Zhou et al., 2020).

To determine if tumor metabolomic profiles are related to patient survival in GBM, we questioned if GBMs can be grouped into different metabolic subtypes with different survival times in a manner similar to efforts to categorize GBMs by transcriptomic and DNA methylation patterns (Ceccarelli et al., 2016; Verhaak et al., 2010).

We first confirmed that our GBM tumor samples reflected a typical clinical cohort by univariate analysis with known survival factors. As expected, older age, male sex, poor performance status, and an unmethylated MGMT promoter were all associated with inferior survival within this cohort of GBM patients (Supplementary Table S1), although some variables did not achieve statistical significance. We then performed unsupervised hierarchical clustering of metabolites in the 40 tumors from GBM patients.

Our cohort included five recurrent GBMs that did not separate from primary GBM by unsupervised hierarchical clustering (Fig. 4A). This analysis identified three unique metabolite-based clusters that stratified GBM tumors into three

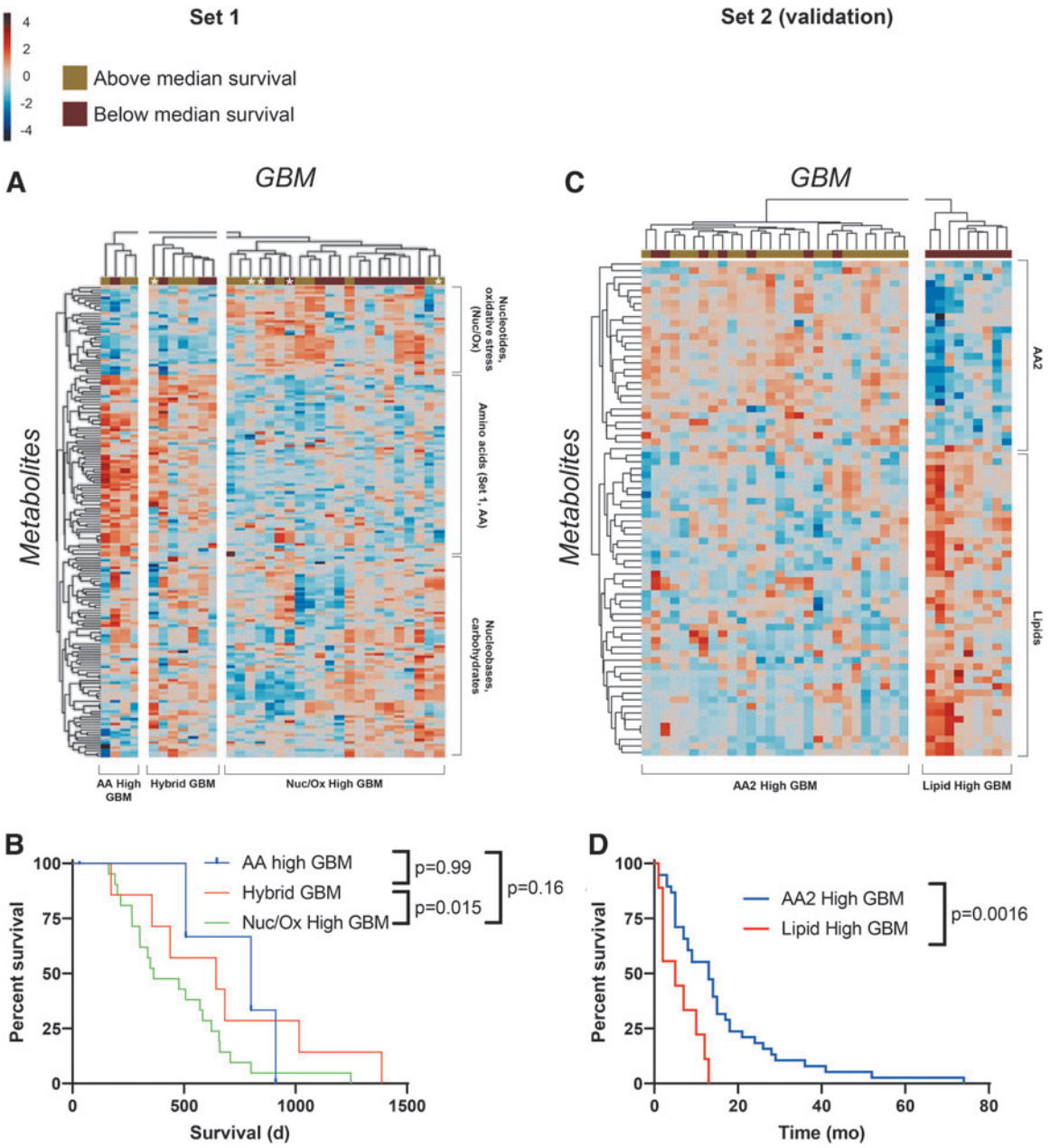

FIG. 4. Metabolomics-based clustering bins GBM patients into groups of different prognosis. (A) Levels of metabolites in GBM patients with known survival times were organized by unsupervised hierarchical clustering. *Indicates recurrent GBM. **(B)** The Kaplan–Meier curves with survival times for patients in the subtypes identified in **(A, C)**. To validate findings in **(A, B)**, a second, independent cohort was assessed using different mass spectrometry methods, and then analyzed by clustering as in **(A, D)**, the Kaplan–Meier curves with survival times for patients in the subtypes identified in **(C)**. Color scales for both heatmaps indicate log-transformed values of data points after normalization to the median AUC of each compound. GBM, glioblastoma.

separate groups (Fig. 4A). Inspection of individual metabolites represented by each metabolite cluster revealed enrichment of either (1) nucleobases and carbohydrates, (2) AAs, or (3) metabolites associated with oxidative stress regulation and mature nucleoside/nucleotide species (Nuc/Ox). We then grouped patients into their three broadest clusters, which varied in general levels of metabolites represented by Nuc/Ox, AA, and nucleobase and carbohydrate metabolites (Fig. 4A).

These three putative metabolic subgroups of GBM comprised of tumors represented by either high levels of metabolites in the AA cluster (AA high GBM), high levels of metabolites in the Nuc/Ox cluster (Nuc/Ox high GBM), or high levels of metabolites in clusters representing AA and carbohydrate/nucleobase metabolites (hybrid GBM). Statistical analyses of these metabolites by ANOVA are shown in Supplementary Data S4. Survival analysis of these three groups had limited statistical power due to our number of patients but indicated prognostic differences associated with this grouping method, with Nuc/Ox-High patients showing the worst survival and the AA group and Nuc/Ox-Low showing superior survival (Fig. 4B).

These differences were not due to receipt of different treatments, as receipt of RT and TMZ was not different between groups (Supplementary Fig. S4A, B). These findings are reminiscent of our previous work, showing that GBMs with high levels of nucleotides and their derivatives, particularly purines, are especially resistant to treatment (Zhou et al., 2020). These data also suggest a potential correlation of high levels of redox metabolites (in the Nuc/Ox-High GBM group) with poor GBM patient survival.

We then asked if survival differences among metabolic subtypes were related to known clinical predictors of GBM patient survival. Assessment of established predictors of GBM patient survival (sex, age at diagnosis, MGMT promoter methylation, performance status, and extent of resection) within each subtype determined a mostly even distribution of these factors across metabolic groups (Supplementary Fig. S4C–G), with no statistical significance when groups were assessed by *t*-test or chi-squared test.

Taken together, these observations indicate that the metabolic features of GBM patient tumors might provide information regarding patient prognosis that could complement the information conveyed by conventionally used clinical information.

To validate our findings that GBMs can cluster into metabolic groups with different prognoses, we assessed a second, independent dataset (validation cohort) of GBM tumor specimens containing both metabolomic profiles and survival times (Chinnaiyan et al., 2012; Kesarwani et al., 2019). While metabolomic data from the validation cohort contained largely different metabolites due to different LC-MS detection methods, patients in the validation cohort could also be binned into metabolically defined subtypes with differing prognosis, consistent with our initial cohort of tumors (Fig. 4C). This analysis was performed with separate metabolomic platforms, and our validation method (performed at a different site) detected only $\sim$60 compounds in common with our in-house method.

Despite differences in detection methods, we were able to find that GBMs containing high levels of groups of AAs in either set had the best prognosis. Consistent with the data obtained using our method, we identified a subtype characterized by an enrichment of AA-related metabolites at above-median levels with superior survival (Fig. 4D). Since our methods utilized different metabolites to discriminate subtypes in the two different patient sets, we refer to this second AA-defined subtype as AA2 to avoid implying biological equivalence with the AA subtype in our independent first dataset.

The second subtype within our validation cohort contained above-median levels of many lipid species and had a significantly reduced median survival compared with the AA2-high subtype. Further statistical analysis identified >140 compounds that differed with $p < 0.05$ between subtypes (Supplementary Fig. S2C). The identification of a lipid-high subtype in this dataset, rather than the Nuc/Ox-related groups reported in set 1, is likely due to differences in LC-MS compound detection methods with limited detection of nucleobases that are increased in patients with worse survival.

Association of individual metabolites with GBM patient survival

Having identified metabolic signatures that correlated with GBM patient survival, we next explored if similar relationships could be seen with *individual* metabolites. For each metabolite in each independent dataset, we determined hazard ratios (Supplementary Fig. S5A, B) and correlation with survival (Supplementary Fig. S5C, D). While a variety of metabolites exceeded the 95% confidence interval, no singular metabolite was reliably associated with survival with a *p*-value of <0.05 in both sets. This may be due to sample quality, different analysis methods across datasets, or the inherently dynamic nature of metabolite levels.

We then asked if GBM patients with below-median *versus* above-median survival were metabolically distinguishable when the two groups were directly compared. To this end, we used partial least-squares discriminant analysis (PLS-DA) to identify metabolic features that could discriminate between above-median survivors and below-median survivors in a supervised manner that incorporates survival information (Fig. 5A, B).

In this comparison, we found that levels of purines including AMP/dGMP and adenine were significantly elevated in patients with inferior survival, and in these patients a variety of other purine and pyrimidine metabolites had increased variable importance in projection (VIP) scores (Fig. 5C). This agrees both with our metabolic clustering (Fig. 4) and with our previous data, showing that purines promote therapeutic resistance in GBM (Zhou et al., 2020). When we assessed our validation cohort, we found that several diverse lipid and AA species were different between groups, in agreement with our metabolic clustering analysis (Fig. 5D). Distinct from these two metabolite categories, levels of ascorbate were notably higher in above-median than in below-median survivors.

Interestingly, redox cofactor ratios did not significantly differ between tumors from patients with above-median and below-median survival (Supplementary Fig. S6A, B). This agrees with our observations that these ratios were similar across glioma types with different median survival times, and suggests that ascorbate metabolism may be a more practical therapeutic target. Indeed, ongoing clinical strategies are aiming to modulate ascorbate levels and improve outcomes in GBM patients (Allen et al., 2019; Schoenfeld et al., 2017).

Metabolomic analysis of primary versus recurrent GBM

Surgical resection and standard chemoradiation therapy improve survival for GBM patients, but this initial efficacy is limited by the development of treatment resistance. Recurrent, therapy-resistant tumors develop within the high-dose radiation field, and the ability of recurrent tumors to resist therapy is in part due to metabolic alterations within the tumor (Scott et al., 2021). Therefore, we asked if recurrent GBMs were metabolically distinct from primary GBM.

Receipt of a second craniotomy in GBM patients is relatively infrequent, and therefore our sample size of recurrent GBM tumors was expectedly smaller ($n = 5$) than that of primary tumors ($n = 35$) and could not achieve an ideal level of confidence for a variety of assessments such as metabolite set enrichment. Examination of unsupervised metabolite clustering data did not identify any clear separation of recurrent from primary GBM (Fig. 4A), nor did supervised clustering of primary and recurrent GBMs produce any obvious metabolite patterns (not shown).

Primary GBM may therefore be less distinguishable from recurrent GBM when compared with the starker metabolic differences observed between IDH wildtype and IDH mutant

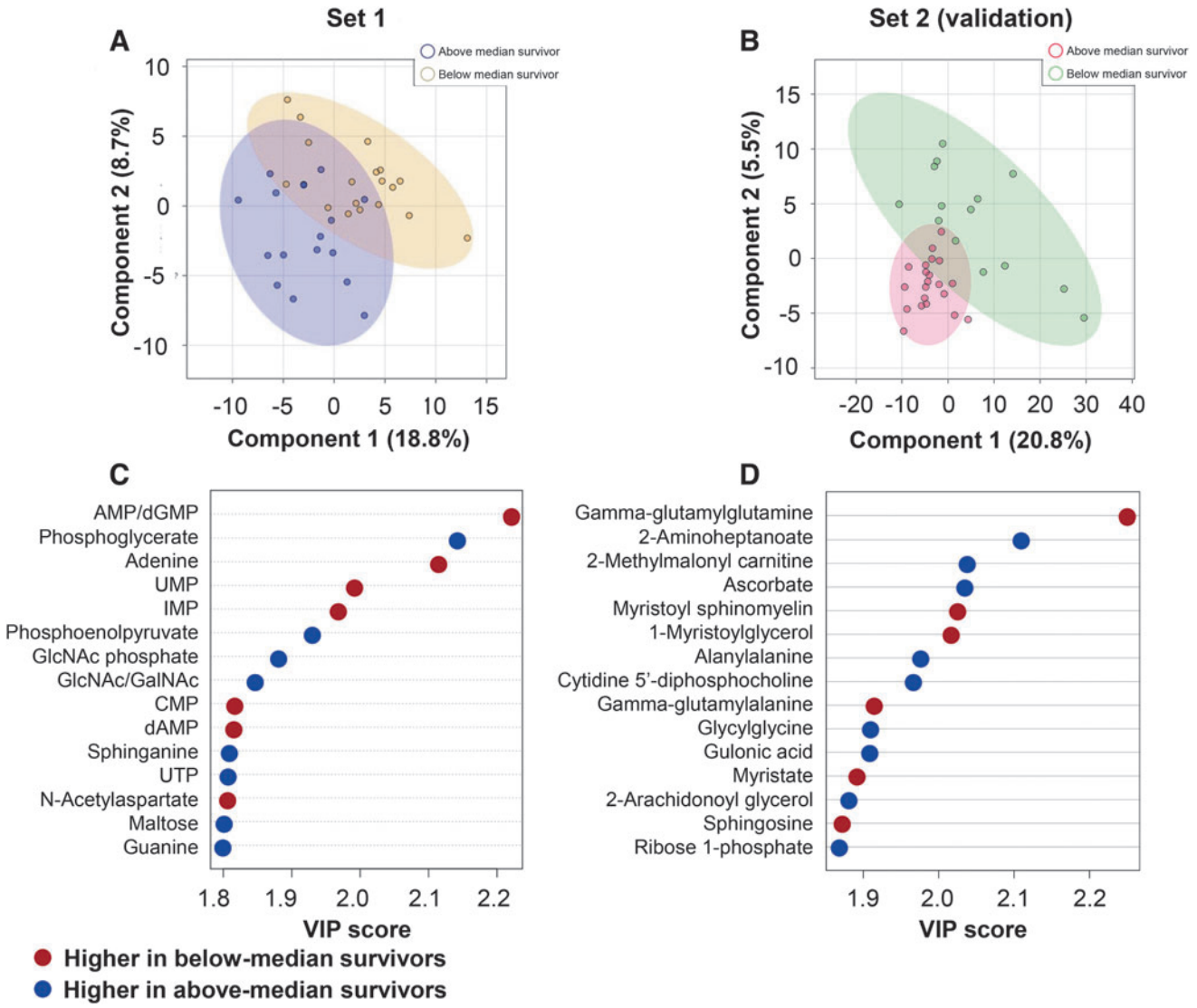

FIG. 5. Assessment of individual metabolites in tumors from GBM patients with different outcomes. (A, B) PLS-DA of independent metabolomics datasets (set 1, experimental; set 2, validation). **(C, D)** VIP scores for metabolites were determined in tumors from below-median *versus* above-median survivors. PLS-DA, partial least-squares discriminant analysis; VIP, variable importance in projection.

gliomas. For example, despite having undergone cycles of RT and chemotherapy, ratios of NAD/NADH and GSH/GSSG were not significantly different in recurrent GBM compared with primary untreated GBM (Supplementary Fig. S7A, B). However, after performing PLS-DA on metabolite data, we noted some separation of primary from recurrent GBMs (Fig. 6A).

Moreover, we identified a variety of interesting metabolites with high VIP scores in recurrent GBM (Fig. 6B). These included a variety of notable purine metabolites that are known to promote GBM treatment resistance (Shireman et al., 2021; Zhou et al., 2020). Levels of guanosine, which may promote glioma stemness, gliomagenesis, and treatment resistance (Kofuji et al., 2019; Shireman et al., 2021; Wang et al., 2017; Zhou et al., 2020), were approximately twice as high in recurrent tumors as in primary GBM (Fig. 6C).

Decreased levels of glutamine and citrate, and increased levels of the pyrimidine metabolite orotate were also observed in recurrent GBM compared with primary GBM (Fig. 6C). These may be promising leads to target metabolic activity in patients with recurrent GBM, and further metabolic and genetic analyses may help experimentally validate pathway activities and directionality.

Validation of metabolic subtypes by transcriptomic analysis

Metabolomic analysis of brain tumors is not a standard part of clinical care, in part due to the logistical challenges of quickly flash-freezing tumor tissue and the cost of metabolomic analysis. We wanted to understand if our metabolism-centric approach to understanding GBM patient outcomes could translate into standard clinical settings where approaches such as exome sequencing and transcriptomic analysis are more commonly performed. Metabolites are linked by the enzymes that catalyze their interconversion, and the levels of these enzymes are quantified in transcriptomic analyses such as RNAseq.

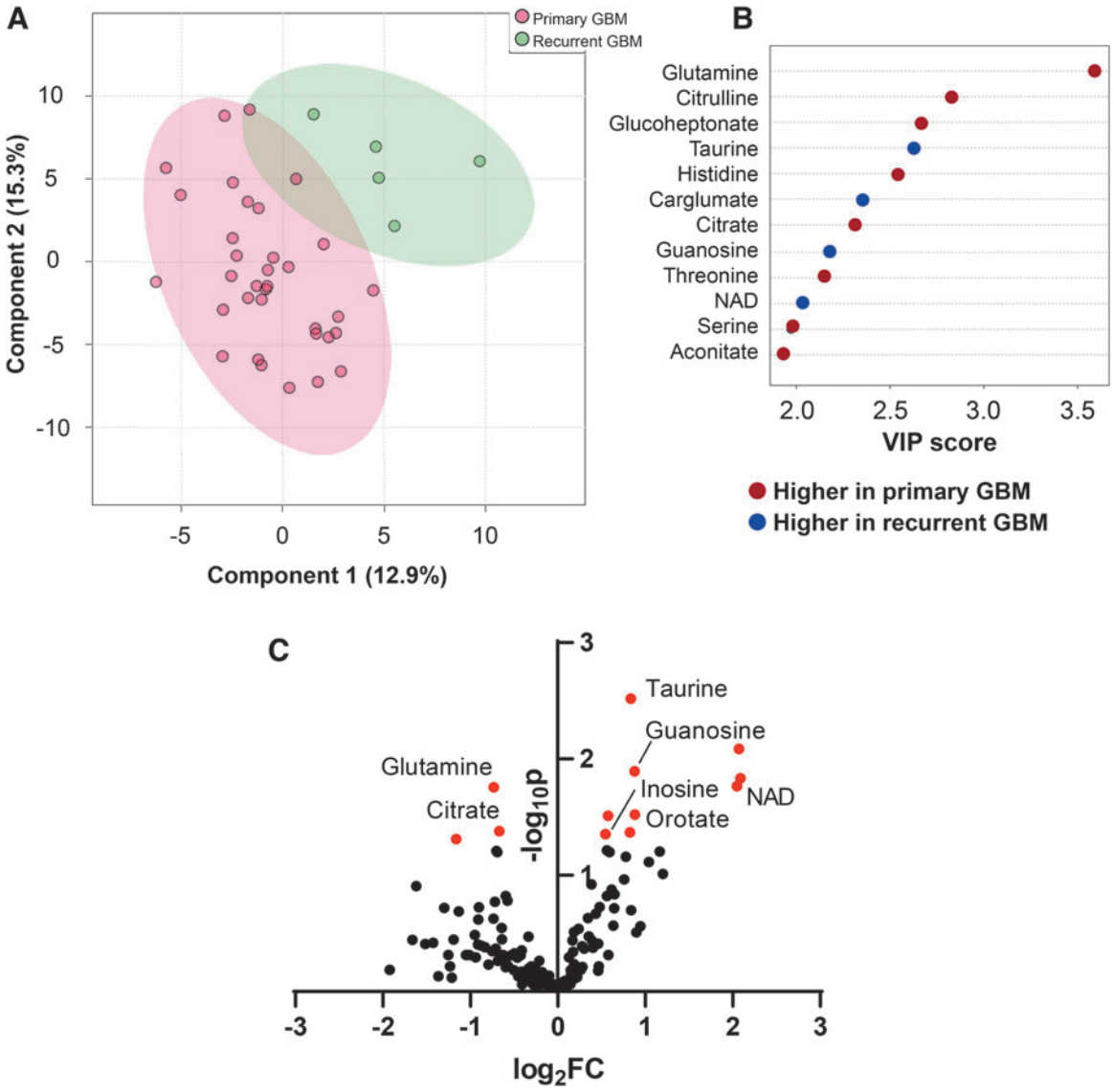

FIG. 6. Metabolomic analyses of primary and recurrent GBM. (A) PLS-DA of a GBM cohort of primary and recurrent tumors. **(B)** VIP scores for metabolites were determined in primary and recurrent GBM tumors. **(C)** Volcano plots of metabolites in primary and recurrent GBMs with *p*-value *versus* FC in abundance (recurrent/primary). Red data points indicate metabolites with *p*-values <0.05. FC, fold change.

We questioned if it were possible to validate metabolic GBM subtypes and their prognostic utility at the transcriptional level. Therefore, we selected the metabolites of each cluster and performed joint pathway analysis with MetaboAnalyst 5.0 (Pang et al., 2021) for each set. This approach allowed us to identify connections globally across gene-metabolite networks and predict the genes likely involved in the metabolic activities of each subtype (Fig. 7A–C, Supplementary Data S5).

We first defined a geneset for each tumor type (Nuc/Ox and AA) comprised of the genes with at least two connections to the respective input metabolites. Thus, these sets of genes were predicted to contribute to tumor metabolic phenotype. We then interrogated linked expression and outcome data from the TCGA to determine how these genesets were associated with GBM patient survival. For each transcriptional signature, TCGA GBM tumor samples were scored using single-sample geneset enrichment analysis (ssGSEA) (Mercatelli et al., 2020), and then assessed for survival in high-scoring (>0) *versus* low-scoring (<0) groups. Similarly, we performed separate analyses of patient survival in each metabolite-defined subtype *versus* the remainder of the cohort.

Comparison of survival curves between metabolite-defined groups and the corresponding transcriptionally defined groups showed close agreement. While statistical power was limited, patients in the Nuc/Ox-high subtype appeared to have inferior survival (Fig. 7D), as did those in the transcriptionally defined Nuc/Ox-high group, although this did not reach statistical significance (Fig. 7E).

While the metabolically defined AA group trended with a higher median survival, the transcriptional AA group showed no significant difference in survival from the rest of the cohort (Fig. 7F, G). Patients in the hybrid subtype had inferior survival (Fig. 7H), consistent with the transcriptionally

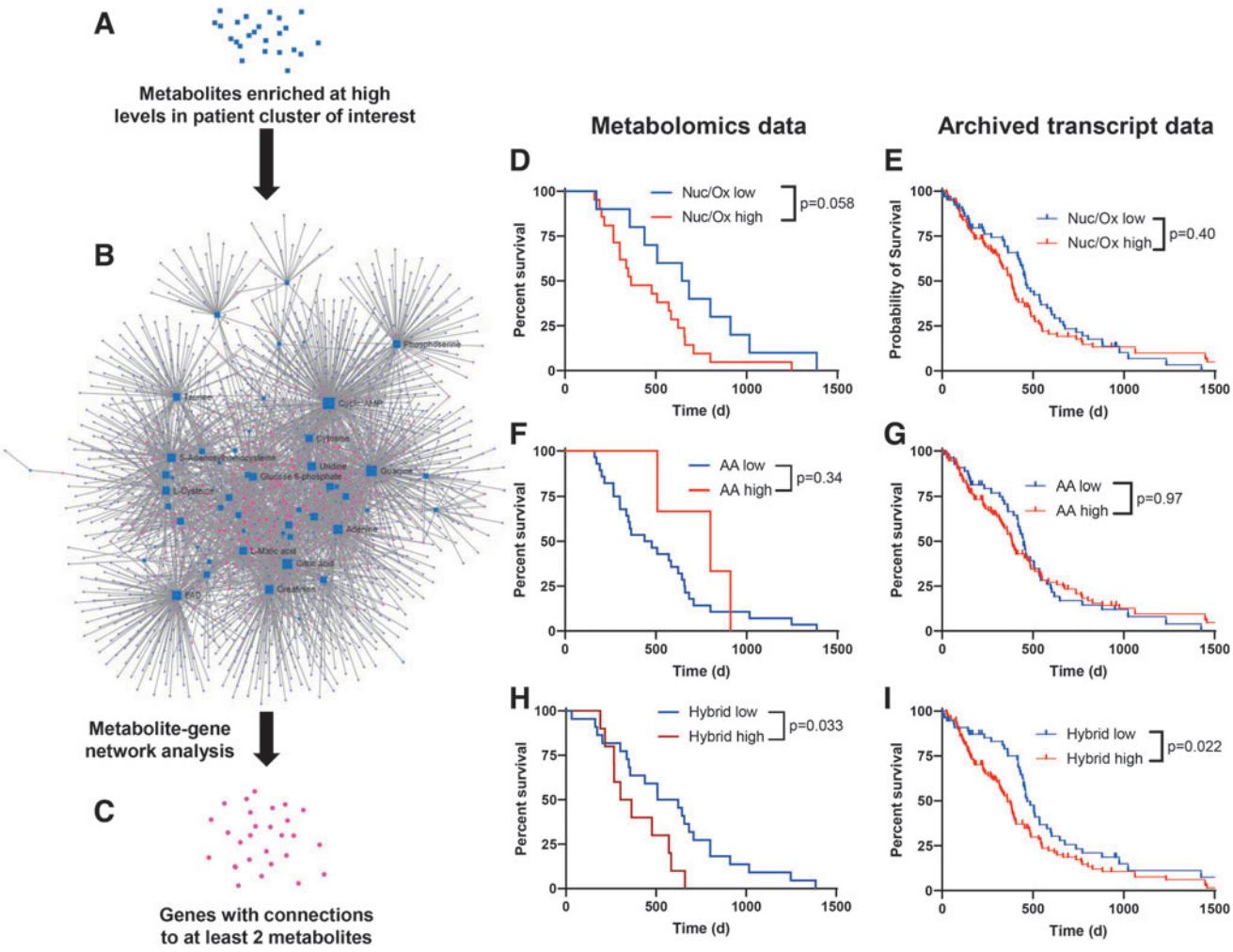

FIG. 7. Transcript validation of GBM metabolic subtypes. **(A)** Metabolites representing each metabolic GBM subtype (with subtype defined as the corresponding patient cluster) were used to identify relevant RNA transcripts by metabolite–gene interactions with high confidence. **(B)** Network of genes and metabolites from metabolite data produced in **(A)**. *Blue squares* represent metabolites; magenta circles represent genes. **(C)** Genes from **(B)** with connections to at least two metabolites were selected for transcriptomic analysis. **(D, F, H)** The Kaplan–Meier curves with patients from the indicated metabolic subtypes (Nuc/Ox, AA, and hybrid GBM) *versus* the remainder of the cohort. **(E, G, I)** The Kaplan–Meier curves using archived transcriptomic data with patients from high *versus* low transcriptomic scores corresponding to the genes identified for each subtype. AA, amino acid; Nuc/Ox, nucleotide and oxidative stress metabolites.

defined group (Fig. 7I). Collectively, these data suggest that gene and metabolite levels of oxidative stress and nucleotide-related metabolites may inform GBM patient prognosis.

Discussion

In this study, we have nominated metabolomic subtypes for GBM that inform patient prognosis and could lead to new treatment strategies. IDHwt GBMs are metabolically separable from IDHmut gliomas, and within the IDHmut group of gliomas grade 4 astrocytomas are metabolically distinct from grade 2 and 3 gliomas. IDHwt GBM and IDHmut gliomas also differ dramatically by 2HG levels, with IDHmut gliomas containing expectedly higher levels than IDHwt GBMs by up to 50-fold. GBMs can be further separated into metabolic groups with different survival times that agree with transcriptional analysis of metabolite-associated genes. These data indicate that metabolic phenotypes of brain tumors may be able to inform patient outcomes and tumor aggressiveness.

There are several general reasons metabolite levels could contribute to patient outcome. Metabolites likely regulate responses to RT and TMZ, which are the predominant treatments prescribed for GBM. For example, high nucleotide levels could provide a readily accessible pool of substrates for nucleic acid synthesis required for proliferation, and/or the production of mature nucleosides and nucleotides that mediate radiotherapy resistance (Zhou et al., 2020).

High levels of carbohydrates might similarly feed anabolic pathways contributing to tumor aggressiveness (Chinnaiyan et al., 2012). We also observed that tumors rich in lipids were linked to worse patient outcomes. This could be explained by numerous cellular activities for lipids, including membrane production in proliferating cells, second messenger activity for proliferative and survival signaling pathways, and

oxidation in the mitochondria to produce redox cofactors and ATP (De Rosa et al., 2012; Lin et al., 2017).

In contrast to carbohydrates, nucleotide species, and lipids, high levels of AAs were associated with more favorable outcomes. Notably, synthesis and degradation pathways of AAs are more diverse, branching about numerous metabolic pathways. Thus, GBMs with high AA levels might represent a more globally active network of metabolic pathways without reserve capacity, and thus may be more easily perturbed by therapy.

Alternatively, or in addition, high AA levels might reflect lower levels of protein synthesis. Both scenarios could in turn lead to more favorable survival. Our observation that predicted genes representing the AA subtype did not correlate with survival (in contrast to metabolite levels) could be explained by several hypotheses. AA pathways represented by the indicated metabolites and transcripts might be regulated post-transcriptionally, in which case transcriptional data would not represent actual metabolic activity. In addition, metabolite levels do not necessarily reflect pathway activity; for example, high AA levels could arise from either increased production or decreased utilization.

At present, metabolomic analysis of patient tumors is infrequently performed in clinical practice. It is costly and logistically difficult to flash-freeze tumor specimens immediately after resection and analyze these specimens by mass spectrometry. There is also a lack of standardization regarding metabolomic detection methods and analysis across academic and medical centers.

We directly observed this difficulty in the different types of metabolites detected between our initial and validation cohorts, which were generated using different platforms. However, further investigation of the metabolic underpinnings of GBM or other cancers might lead to standardized diagnostic and prognostic methods for metabolite detection and quantification. Beginning to address these issues would likely involve immediate flash freezing of tissue after resection to prevent *ex vivo* metabolic activity (*e.g.,* conversions of redox cofactors), and/or infusions with metabolic tracers such as nonradioactive isotopic glucose to predict *in vivo* activity.

The identification of specific biomarkers and direct measurements of their levels in blood or solid tissue are ideal, but emerging methods in artificial intelligence and metabolic flux analysis could be used to define metabolic pathway activity more comprehensively in animal models and humans (Giera et al., 2022; Patti et al., 2012). Studies employing analysis of transcriptional or proteomic signatures with patient-matched metabolomic data could identify molecular profiles that directly correspond to metabolic subtype. Such a profile could be used to predict metabolic treatments that are effective against specific GBM tumor types.

From a therapeutic targeting perspective, numerous metabolic inhibitors could be tailored to specific GBM metabolic groups. Classical examples include gemcitabine and fluorouracil, which suppress nucleotide metabolism and nucleic acid synthesis (Scott et al., 2021). More recent examples that we and others are investigating include the FDA-approved inosine monophosphate dehydrogenase inhibitor known as mycophenolate mofetil (MMF (Majd et al., 2014)), which is used to block purine synthesis in autoimmunity and is under investigation in GBM (NCT04477200).

This may be an especially effective novel therapy in the Nuc/Ox subgroup, which is high in nucleotides. GBMs in the AA/AA2 subtypes might be treated with AA-targeted approaches such as the glutamine antagonist JHU-083, asparaginase, or a methionine-restricted diet (Gao et al., 2019; Hanaford et al., 2019; Karpel-Massler et al., 2016). Lipid metabolism can be targeted by etomoxir or statins, and might be an effective approach against GBMs rich in lipids, which may encompass the Nuc/Ox-defined GBMs (Kant et al., 2020).

Our data further suggest that metabolic phenotypes in patients could mediate resistance to standard therapies. Radiotherapy, a standard treatment for GBM, causes DNA damage and oxidative stress. Notably, oxidative stress can be targeted by pharmacological ascorbate, which has shown early promise in patients (Allen et al., 2019). It could be speculated that ascorbate treatment may be most effective in Nuc/Ox-high GBMs and recurrent GBM, which is likely to have higher levels of oxidative stress.

While our analyses define subsets of human GBM by metabolite *levels*, metabolic pathway *activity* remains to be defined across subtypes. This can be accomplished by measuring the accumulation of an isotope tracer (*e.g.*, ^{13}C-glucose) into downstream intermediates. Stable isotope tracing is feasible in both preclinical animal models and cancer patients (Bartman et al., 2021; Faubert et al., 2021), and could potentially be used in this endeavor.

Finally, determining the molecular mechanisms of these phenotypic differences, and how they contribute to tumor progression and therapy resistance, across subtypes *in vitro* and in preclinical animal models will be critical to translation into clinical care. Altogether, these metabolic analyses suggest that gliomas can be grouped into distinct survival groups by metabolite levels and could lay the groundwork to begin developing novel therapeutic strategies for glioma patients.

Materials and Methods

Patients, tissue collection and storage

For >10 years, the Neurosurgery Department at the University of Michigan has processed and stored resected brain tumor samples not needed for clinical use to facilitate future research endeavors. All samples in this brain tumor bank undergo quality assurance by a clinical neuropathologist to estimate viability and tumor content. Due to the need for banked tissue, patients who only underwent diagnostic biopsy rather than tumor resection are not included in this analysis. Among the types of tissues collected was flash-frozen brain tumor tissue appropriate for metabolomic analysis. Clinical information linked to these samples was abstracted from the medical record under an IRB-approved research protocol (HUM00165469).

IDH profiling and tumor type assignment

IDH status and molecular analysis of resected tumors were determined by the University of Michigan Neuropathology Unit according to standard clinical practice. IDH mutations were determined by immunohistochemistry for the R132 mutant of IDH1 and/or PCR (Supplementary Data S2). IDHmut oligo were defined as tumors having both IDH mutation and deletions of chromosomal arms 1p and 19q,

while IDHmut astro were defined as those with the IDH mutation without chromosomal deletion of 1p and 19q. Adult diffuse infiltrating gliomas without the IDHmut were classified as IDHwt GBM.

Sample preparation

Frozen tissue specimens were homogenized in cold (−80°C) 80% methanol. Soluble metabolite fractions were separated from insoluble homogenate by centrifugation and dried by speedvac at volumes normalized to equal tissue weights. Dried metabolites were then reconstituted in 1:1 methanol:water for LC-MS.

Liquid chromatography-mass spectrometry

Metabolite extracts were analyzed using an Agilent Technologies Triple Quad 6470 LC-MS/MS system consisting of the 1290 Infinity II LC Flexible Pump (Quaternary Pump), the 1290 Infinity II Multisampler, the 1290 Infinity II Multicolumn Thermostat with 6 port valve, and the 6470 triple quad mass spectrometer. Agilent MassHunter Workstation Software LC/MS Data Acquisition for 6400 Series Triple Quadrupole MS with Version B.08.02 was used for compound optimization, calibration, and data acquisition. Chromatographic separation of compounds is as described (Zhou et al., 2020).

Data were preprocessed with Agilent MassHunter Workstation QqQ Quantitative Analysis Software (B0700). For all compounds, the extracted ion chromatograms and mass spectra were manually inspected for sample quality and consistent peak integrations. To validate findings, a second set of samples from patients of an independent cohort (Chinnaiyan et al., 2012; Kesarwani et al., 2019) was assessed by mass spectrometry by Metabolon.

Statistical analysis

Descriptive statistics were used to characterize baseline patient and treatment characteristics. Univariable Cox proportional hazard models were used to estimate the association between clinical factors (age and year of diagnosis, performance status, MGMT methylation status, extent of resection, and gender) and overall survival. Kendall's tau for censored data was used to rank the correlation between metabolites and overall survival. All analyses, described in detail below, were performed using MetaboAnalyst 5.0, GraphPad Prism 8.0.0, and R 4.2.2.

Metabolomic analysis

Unsupervised hierarchical clustering, heat map generation, and PLS-DA were performed using MetaboAnalyst 5.0 (Pang et al., 2021). Processed peak intensities were normalized by the median of all samples, log-transformed (base 10), and used to generate metabolite-based patient groups by unsupervised hierarchical clustering (Euclidian clustering and Ward distance). All detected metabolites after LC-MS data redundancy correction (below) were used to produce the heatmap representing patient cohort 1, and the 75 metabolites with the lowest *p*-values were used to produce the heatmap representing the independent validation cohort 2.

Metabolic subtypes were defined as the predominant patient clusters encompassing all GBM samples. Metabolites representing each subtype were identified from the largest clusters covering all metabolites detected. Network analysis was performed on metabolites representing each subtype and using the joint gene–metabolite interaction network module. Metabolite–gene associations were retrieved from STITCH (Kuhn et al., 2008).

Reduction of LC-MS data with Binner

Metabolite features generated from our metabolomics platform were subjected to Binner quality control analysis (Kachman et al., 2019). In brief, metabolite features were binned by retention time, and Pearson's correlation of intensity values was calculated for each feature bin. Isotopes were identified by retention time similarity, correlation, and mass differences. After isotope detection, metabolites in each bin are clustered by correlation coefficients of signal intensities.

For each cluster, the highest intensity feature is treated as a neutral mass and iteratively assigned adducts corresponding to the most frequent ions (*e.g.,* m+H, m+Na). Calculated adducts for each metabolite are searched within the bin based on the m/z of other features in the cluster. Identified adducts were removed from the dataset.

Transcriptional analysis

HTseq quantified RNAseq counts data for 173 TCGA GBM samples available in the GDC TCGA Glioblastoma cohort (https://xenabrowser.net/datapages) were downloaded from the UCSC Xena browser (Goldman et al., 2020). Survival data for these cases were obtained from the TCGA Clinical Data Resource (Liu et al., 2018). Enrichment scores of each case for specific metabolic genesets were computed with the ssGSEA function in the corto R package version 1.1.11 (Mercatelli et al., 2020). We split cases based on positive or negative enrichment scores for the genesets and visualized their survival differences using the Kaplan–Meier method with *p*-values computed using the log-rank test.

Authors' Contributions

A.J.S., L.O.C, C.A.L, and D.R.W contributed to writing; all authors performed review and editing; A.J.S., L.O.C, D.M.E, Y.S., V. R., A.C.A, L.Z, S.S., N.J., S.A.C., A.R., C.A.L, and D.R.W. provided methodology and data analysis; A.J.S., L.O.C, C.A.L., and D.R.W. designed conceptualization; K.V., K.M., O.S., S.H.J., D.O., M.M.K., L.J., Y.U., D.L., S.V., S.C.P., T.S.L., J.E.I., W.N.A., P.C., J.H., and D.R.W assisted with sample procurement and analysis.

Author Disclosure Statement

None of the authors have relevant conflicts of interest to disclose.

Funding Information

A.J.S. was supported by the NCI (F32CA260735); L.O.C. was supported by the NCI (T32CA140044) and the NIAID

(T32AI007413); S.A.C. was supported by the Rogel Cancer Center Core Grant and the Dr. Frank Limpert Career Development Fund at the University of Michigan Rogel Cancer Center; D.O. was supported by the NCI (R01CA226527); J.E.I. was supported by the NCI (K99/R00CA218869 and R21CA242221); P.C. was supported by the NINDS (R01NS110838 and R21NS090087), American Cancer Society grant RSG-11–029-01, and Bankhead-Coley Cancer Research Program; A.R. was supported by the NCI (R37CA214955), MIDAS PODS grant, MICDE Catalyst grant, and institutional startup funds from the University of Michigan Ann Arbor; C.A.L. was supported by the NCI (R01CA244931) and UMCCC Core Grant (P30CA046592); D.R.W. was supported by the NCI (K08CA234416 and R37CA258346), Cancer Center Support Grant P30CA46592, Damon Runyon Cancer Foundation, Ben and Catherine Ivy Foundation, and the Sontag Foundation.

Supplementary Material

Supplementary Data S1
Supplementary Data S2
Supplementary Data S3
Supplementary Data S4
Supplementary Data S5
Supplementary Figure S1
Supplementary Figure S2
Supplementary Figure S3
Supplementary Figure S4
Supplementary Figure S5
Supplementary Figure S6
Supplementary Figure S7
Supplementary Table S1

References

Allen BG, Bodeker KL, Smith MC, et al. First-in-Human Phase I Clinical Trial of Pharmacologic Ascorbate Combined with Radiation and Temozolomide for Newly Diagnosed Glioblastoma. Clin Cancer Res 2019;25(22):6590–6597; doi: 10.1158/1078-0432.Ccr-19-0594

Bartman CR, Teslaa T, Rabinowitz JD. Quantitative flux analysis in mammals. Nat Metab 2021;3(7):896–908.

Brat DJ, Aldape K, Colman H, et al. cIMPACT-NOW update 5: Recommended grading criteria and terminologies for IDH-mutant astrocytomas. Acta Neuropathol 2020;139(3):603–608; doi: 10.1007/s00401-020-02127-9

Ceccarelli M, Barthel FP, Malta TM, et al. Molecular profiling reveals biologically discrete subsets and pathways of progression in diffuse glioma. Cell 2016;164(3):550–563; doi: 10.1016/j.cell.2015.12.028

Chinnaiyan P, Kensicki E, Bloom G, et al. The metabolomic signature of malignant glioma reflects accelerated anabolic metabolism. Cancer Res 2012;72(22):5878–5888; doi: 10.1158/0008-5472.can-12-1572-t

Dang L, White DW, Gross S, et al. Cancer-associated IDH1 mutations produce 2-hydroxyglutarate. Nature 2009; 462(7274):739–744; doi: 10.1038/nature08617

De Rosa A, Pellegatta S, Rossi M, et al. A radial glia gene marker, fatty acid binding protein 7 (FABP7), is involved in proliferation and invasion of glioblastoma cells. PLoS One 2012;7(12):e52113; doi: 10.1371/journal.pone.0052113

Eckel-Passow JE, Lachance DH, Molinaro AM, et al. Glioma Groups Based on 1p/19q, IDH, and TERT Promoter Mutations in Tumors. N Engl J Med 2015;372(26):2499–2508; doi: 10.1056/NEJMoa1407279

Faubert B, Tasdogan A, Morrison SJ, et al. Stable isotope tracing to assess tumor metabolism in vivo. Nat Protoc 2021; 16(11):5123–5145; doi: 10.1038/s41596-021-00605-2

Gao X, Sanderson SM, Dai Z, et al. Dietary methionine influences therapy in mouse cancer models and alters human metabolism. Nature 2019;572(7769):397–401; doi: 10.1038/s41586-019-1437-3

Giera M, Yanes O, Siuzdak G. Metabolite discovery: Biochemistry's scientific driver. Cell Metab 2022;34(1):21–34; doi: 10.1016/j.cmet.2021.11.005

Goldman MJ, Craft B, Hastie M, et al. Visualizing and interpreting cancer genomics data via the Xena platform. Nat Biotechnol 2020;38(6):675–678; doi: 10.1038/s41587-020-0546-8

Hanaford AR, Alt J, Rais R, et al. Orally bioavailable glutamine antagonist prodrug JHU-083 penetrates mouse brain and suppresses the growth of MYC-driven medulloblastoma. Transl Oncol 2019;12(10):1314–1322; doi: 10.1016/j.tranon.2019.05.013

Hanahan D. Hallmarks of cancer: New dimensions. Cancer Discov 2022;12(1):31–46; doi: 10.1158/2159-8290.cd-21-1059

Hartmann C, Meyer J, Balss J, et al. Type and frequency of IDH1 and IDH2 mutations are related to astrocytic and oligodendroglial differentiation and age: A study of 1,010 diffuse gliomas. Acta Neuropathol 2009;118(4):469–474; doi: 10.1007/s00401-009-0561-9

Kachman M, Habra H, Duren W, et al. Deep annotation of untargeted LC-MS metabolomics data with Binner. Bioinformatics 2019;36(6):1801–1806; doi: 10.1093/bioinformatics/btz798

Kant S, Kesarwani P, Prabhu A, et al. Enhanced fatty acid oxidation provides glioblastoma cells metabolic plasticity to accommodate to its dynamic nutrient microenvironment. Cell Death Dis 2020;11(4):253; doi: 10.1038/s41419-020-2449-5

Karpel-Massler G, Ramani D, Shu C, et al. Metabolic reprogramming of glioblastoma cells by L-asparaginase sensitizes for apoptosis in vitro and in vivo. Oncotarget 2016;7(23): 33512–33528; doi: 10.18632/oncotarget.9257

Kesarwani P, Prabhu A, Kant S, et al. Metabolic remodeling contributes towards an immune-suppressive phenotype in glioblastoma. Cancer Immunol Immunother 2019;68(7): 1107–1120; doi: 10.1007/s00262-019-02347-3

Kofuji S, Hirayama A, Eberhardt AO, et al. IMP dehydrogenase-2 drives aberrant nucleolar activity and promotes tumorigenesis in glioblastoma. Nat Cell Biol 2019; 21(8):1003–1014; doi: 10.1038/s41556-019-0363-9

Kuhn M, Von Mering C, Campillos M, et al. STITCH: Interaction networks of chemicals and proteins. Nucleic Acids Res 36(Database issue)2008;:D684–D688; doi: 10.1093/nar/gkm795

Lai A, Kharbanda S, Pope WB, et al. Evidence for sequenced molecular evolution of IDH1 mutant glioblastoma from a distinct cell of origin. J Clin Oncol 2011;29(34):4482–4490; doi: 10.1200/JCO.2010.33.8715

Lee HJ, Kremer DM, Sajjakulnukit P, et al. A large-scale analysis of targeted metabolomics data from heterogeneous biological samples provides insights into metabolite dynamics. Metabolomics 2019;15(7):103; doi: 10.1007/s11306-019-1564-8

Lin H, Patel S, Affleck VS, et al. Fatty acid oxidation is required for the respiration and proliferation of malignant gli-

oma cells. Neuro Oncol 2017;19(1):43–54; doi: 10.1093/neuonc/now128
Liu J, Lichtenberg T, Hoadley KA, et al. An Integrated TCGA Pan-cancer clinical data resource to drive high-quality survival outcome analytics. Cell 2018;173(2):400–416; doi: 10.1016/j.cell.2018.02.052
Louis DN, Perry A, Reifenberger G, et al. The 2016 World Health Organization Classification of Tumors of the Central Nervous System: A summary. Acta Neuropathol 2016; 131(6):803–820; doi: 10.1007/s00401-016-1545-1
Louis DN, Perry A, Wesseling P, et al. The 2021 WHO classification of tumors of the central nervous system: A summary. Neuro Oncol 2021;23(8):1231–1251; doi: 10.1093/neuonc/noab106
Majd N, Sumita K, Yoshino H, et al. A review of the potential utility of mycophenolate mofetil as a cancer therapeutic. J Cancer Res 2014;2014:1–12; doi: 10.1155/2014/423401
Mercatelli D, Lopez-Garcia G, Giorgi FM. Corto: A lightweight R package for gene network inference and master regulator analysis. Bioinformatics 2020;36(12):3916–3917; doi: 10.1093/bioinformatics/btaa223
Pang Z, Chong J, Zhou G, et al. MetaboAnalyst 5.0: Narrowing the gap between raw spectra and functional insights. Nucleic Acids Res 2021;49(W1):W388–W396; doi: 10.1093/nar/gkab382
Parsons DW, Jones S, Zhang X, et al. An integrated genomic analysis of human glioblastoma multiforme. Science 2008; 321(5897):1807–1812; doi: 10.1126/science.1164382
Patti GJ, Yanes O, Siuzdak G. Innovation: Metabolomics: The apogee of the omics trilogy. Nat Rev Mol Cell Biol 2012; 13(4):263–269; doi: 10.1038/nrm3314
Prabhu AH, Kant S, Kesarwani P, et al. Integrative cross-platform analyses identify enhanced heterotrophy as a metabolic hallmark in glioblastoma. Neuro Oncol 2019;21(3): 337–347; doi: 10.1093/neuonc/noy185
Schoenfeld JD, Sibenaller ZA, Mapuskar KA, et al. O2(-) and H2O2-Mediated Disruption of Fe Metabolism Causes the Differential Susceptibility of NSCLC and GBM cancer cells to pharmacological ascorbate. Cancer Cell 2017;32(2):268; doi: 10.1016/j.ccell.2017.07.008
Schwarz JK, Siegel BA, Dehdashti F, et al. Association of posttherapy positron emission tomography with tumor response and survival in cervical carcinoma. JAMA 2007; 298(19):2289–2295; doi: 10.1001/jama.298.19.2289
Scott AJ, Lyssiotis CA, Wahl DR. Clinical targeting of altered metabolism in high-grade glioma. Cancer J 2021;27(5):386–394; doi: 10.1097/ppo.0000000000000550
Shenouda G, Souhami L, Petrecca K, et al. A Phase 2 Study of Neo-adjuvant Metformin and Temozolomide followed by Hypofractionated Accelerated RadioTherapy (HART) with Concomitant and Adjuvant Metformin and Temozolomide (TMZ) in Patients with Glioblastoma. Int J Radiat Oncol Biol Phys 2020;108(3):S21; doi: 10.1016/j.ijrobp.2020.07.2107
Shi DD, Savani MR, Levitt MM, et al. De novo pyrimidine synthesis is a targetable vulnerability in IDH mutant glioma. Cancer Cell 2022;40(9):939–956; doi: 10.1016/j.ccell.2022.07.011
Shireman JM, Atashi F, Lee G, et al. De novo purine biosynthesis is a major driver of chemoresistance in glioblastoma. Brain 2021;144(4):1230–1246; doi: 10.1093/brain/awab020
Suchorska B, Jansen NL, Linn J, et al. Biological tumor volume in 18FET-PET before radiochemotherapy correlates with survival in GBM. Neurology 2015;84(7):710–719; doi: 10.1212/wnl.0000000000001262
Tesileanu CMS, Sanson M, Wick W, et al. Temozolomide and Radiotherapy versus Radiotherapy Alone in Patients with Glioblastoma, IDH-wildtype: Post Hoc Analysis of the EORTC Randomized Phase III CATNON Trial. Clin Cancer Res 2022;28(12):2527–2535; doi: 10.1158/1078-0432.Ccr-21-4283
Verhaak RGW, Hoadley KA, Purdom E, et al. Integrated genomic analysis identifies clinically relevant subtypes of glioblastoma characterized by abnormalities in PDGFRA, IDH1, EGFR, and NF1. Cancer Cell 2010;17(1):98–110; doi: 10.1016/j.ccr.2009.12.020
Wang X, Yang K, Wu Q, et al. Targeting pyrimidine synthesis accentuates molecular therapy response in glioblastoma stem cells. Sci Transl Med 2019;11(504):eaau4972; doi: 10.1126/scitranslmed.aau4972
Wang X, Yang K, Xie Q, et al. Purine synthesis promotes maintenance of brain tumor initiating cells in glioma. Nat Neurosci 2017;20(5):661–673; doi: 10.1038/nn.4537
Zhou W, Yao Y, Scott AJ, et al. Purine metabolism regulates DNA repair and therapy resistance in glioblastoma. Nat Commun 2020;11(1):3811; doi: 10.1038/s41467-020-17512-x

Address correspondence to:
Dr. Costas A. Lyssiotis
Rogel Cancer Center
University of Michigan
Ann Arbor, MI 48109
USA

E-mail: clyssiot@med.umich.edu

Dr. Daniel R. Wahl
Department of Radiation Oncology
University of Michigan
Ann Arbor, MI 48109
USA

E-mail: dwahl@med.umich.edu

Date of first submission to ARS Central, June 15, 2022; date of final revised submission, February 7, 2023; date of acceptance, February 7, 2023.

Abbreviations Used

AA = amino acid
AMP = adenosine monophosphate
ATP = adenosine triphosphate
AUC = area under curve
CMP = cytidine monophosphate
dAMP = deoxyadenosine monophosphate
dCMP = deoxycytidine monophosphate
dGMP = deoxyguanosine monophosphate
GalNAc = N-acetylgalactosamine
GBM = glioblastoma
GlcNAc = N-acetylglucosamine
GSH = reduced glutathione
GSSG = oxidized glutathione

Abbreviations Used (Cont.)

IDH = isocitrate dehydrogenase
IDHmut astro = IDHmut astrocytoma
IDHmut oligo = IDHmut oligodendroglioma
IDHmut = IDH-mutant
IDHwt = IDH-wildtype
IMP = inosine monophosphate
LC-MS = liquid chromatography-mass spectrometry
MGMT = O^6-methylguanine-DNA methyltransferase
NAD = nicotinamide adenine dinucleotide
NADH = reduced nicotinamide adenine dinucleotide
NMN = nicotinamide mononucleotide
Nuc/Ox = nucleotide and oxidative stress metabolites
PLS-DA = partial least-squares discriminant analysis
RT = radiation therapy
ssGSEA = single-sample geneset enrichment analysis
TMZ = temozolomide
UMAP = uniform manifold approximation and projection
VIP = variable importance in projection